The *Aspergillus* aquaglyceroporin gene *AgGlpF* confers high osmosis tolerance in heterologous organisms

Xiao-Dan Liu[a,b], Yi Wei[a], Xiao-Yang Zhou[a], Xue Pei[a], Shi-Hong Zhang[a]#

[a]College of Plant Sciences, Jilin University, Changchun, China

[b]Current address: Institute of Bioengineering, Jilin Agriculture Science and Technology College, Jilin, China

#Address correspondence to Shi-Hong Zhang via E-mail zhang_sh@jlu.edu.cn, telephone +86-431-87836274, or fax +86-431-87835708.

Running Head: *AgGlpF*s confers high osmosis tolerance

ABSTRACT

Aquaglyceroporins (GlpFs) that transport glycerol along with water and other uncharged solutes are involved in osmoregulation in myriad species. Fungal species form a large group of eukaryotic organisms, and their GlpFs may be diverse with various actions. However, few filamentous fungal GlpFs have been biologically investigated. Here, a *GlpF* gene from the halophilic fungus *Aspergillus glaucus* (*AgGlpF*) has been verified to be a channel of water or glycerol in *Xenopus laevis* Oocytes, and been further functionally analyzed in three heterologous systems. In *Saccharomyces cerevisiae*, cells overexpressing *AgGlpF* possessed significant tolerance to drought, salt, and certain metal ions. Then *AgGlpF* was characterized in the filamentous fungus of *Neurospora crassa*. Based on the *NcAQP* disruption mutant (Δ*aqp*), a series of complementary strains of *NcAQP*, *AgGlpF* and three *NPA*-deleted *AgGlpF* fragments were created. Through salt resistant analysis, the *AgGlpF* complementary strain possessed the highest salt-resistant ability among the tested strains. In addition, the intracellular glycerol content in the *AgGlpF* complementary strain was markedly higher than that in the other strains. The AgGlpF-GFP fusion protein was subcellularly localized in the plasma membrane of onion epidermal cells, suggesting that *AgGlpF* functions in plants. Indeed, when *AgGlpF* was expressed in *Arabidopsis thaliana*, transgenic lines survived under high osmotic stress, and particularly under drought stress. Overall, our results revealed that AgGlpF as a water/glycerol transporter is required for survivals of both fungi and plants under high

osmotic stress and may have application values in genetic engineering for generating high salt and drought resistance.

INTRODUCTION

Aquaporins (AQPs) belong to the superfamily of major intrinsic proteins (MIPs), which are membrane water/glycerol channels involved in many physiological processes. The primary function of MIPs is to facilitate the bidirectional transfer of water and small solutes across biological membranes in response to osmotic gradients (1). The AQPs are membrane channels that have been widely detected in most organisms, from bacteria and fungi to plants and animals (2). According to their permeability and structure, aquaglyceroporins (AQGPs) has been separated from AQPs.

The water permeability of plasma membranes was a strong focus in AQP research until the first member of a solute transporter, the *Escherichia coli* glycerol facilitator (GlpF), was discovered (3) and functionally characterized (4). The *E. coli* GlpF is responsible for water and solute transport across the cell membrane (5-10), and its crystal structure at a 2.2 Å resolution has been well described (11).

In yeasts and filamentous fungi, AQGPs can be initially divided into three major branches: FPS1-like, Yfl054-like, and other AQGPs (12). FPS1-like proteins are found only in yeast and the other AQGPs only in filamentous fungi, whereas Yfl054-like proteins are found in both yeasts and filamentous fungi (12). The other major subgroups of fungal AQGPs are classified as α and β and are found in *Ascomycota* and *Basidiomycota*, respectively (13). There are two small fungal AQGP subgroups

designated γ1 and γ2. The γ1 is mainly found in species of *Mucoromycotina*. The second cluster, γ2, is newly recognized to be in filamentous *Ascomycota* (14).

AQGPs in fungi are diverse and possess a large number of subgroups, but relatively few filamentous fungal AQGPs have been functionally analyzed. Instead, those of the yeast *Saccharomyces cerevisiae* have been the most thoroughly studied. The two genes encoding AQGPs in the yeast genome, Fps1 (15,16) and Yfl054 (16,17), are functional glycerol facilitators. Fps1 play a key role in yeast osmoregulation by regulating intracellular glycerol levels during changes in external osmolarity (18-20), whereas the cellular function of Yfl054 remains uncertain (16).

Recently, AQGPs from the arbuscular mycorrhizal fungus have been paid more attention to. The aquaglyceroporin GintAQPF2 from *Glomus intraradices*, a member of the γ subgroup (13), showed high activity when exposed to polyethylene glycol and high capacity to transport water, which is crucial for transformed yeast cells to survive osmotic stress (21). Similarly, two AQGPs (Lacbi1:317173 and 391485) in the ectomycorrhizal basidiomycete *Laccaria bicolor*, belonging to the α subgroup (13), enabled much higher water permeability than did the orthodox AQP Lacbi1:392091 (22). Lacbi1:317173 and Lacbi1:391485 also enabled ammonia (Lacbi1:391485 also enabled glycerol) permeability, which might be responsible for nitrogen efflux in ectomycorrhiza symbiosis (23).

In the genome of the rice blast fungus *Magnaporthe oryzae*, four orthodox AQPs and one AQGP of clusters II and III each have been deduced

(http://genome.jgi.doe.gov/Maggr1/Maggr1.home.html); and three of these genes were upregulated in the infection structure of appressoria (24). Aquaglyceroporin-mediated glycerol efflux from appressoria might be essential in *M. oryzae* after plant cell wall penetration to avoid cells bursting. Indeed, glycerol accumulation has also been shown to be essential for plant cell infections (25).

Plant AQPs perform versatile functions in water uptake, nutrient balancing, nutrient/heavy metal acquisition, and seed development. Actually, plant AQPs also function to modulate abiotic stress-induced signaling (26). In plant, AQPs comprise four major groups on the basis of their localizations: plasma membrane intrinsic proteins, tonoplast intrinsic proteins, NOD26-like intrinsic proteins, and small basic intrinsic proteins. In addition to water, plant AQPs are also known to transport CO_2, H_2O_2, urea, ammonia, silicic acid, arsenite, and a wide range of small uncharged solutes. The NOD26-like intrinsic proteins have glycerol transport activity (27) and thus can be regarded as plant glycerol transporters.

To date, 13 of AQPs have been well studied in mammalian tissues (AQP0–AQP12). Among them, AQP3, AQP7, AQP9, and AQP10 belong to the subset of AQGPs that allow the permeation of water, glycerol, and other small molecules. AQP7 has long been believed to be the only aquaglyceroporin associated with adipose tissue. AQP7 facilitates the efflux of glycerol from adipose tissue, and an AQP7 deficiency has been linked to triglyceride accumulation in adipose tissue and adult onset obesity. The main physiological functions of AQP3 are skin hydration and renal urine concentration (28,29).

AQP9 expressed in liver facilitates the hepatic uptake of glycerol and thus the availability of glycerol for de novo synthesis of glucose and triglyceride, which are both involved in the pathophysiology of diabetes. AQP10 is abundantly expressed in the human duodenum, jejunum, and ileum, contributing to intestinal water and glycerol absorption (30,31).

Studies to date on cellular functions of AQGPs in filamentous fungi are relatively scarce, though filamentous species form a large group of eukaryotic organisms. Previously, we isolated the halophilic fungus *Aspergillus glaucus* from air-dried wild vegetation at the surface periphery of a solar salt field (32). This species shows extreme salt tolerance, with a salinity range for growth from 5 to 32% (saturation) NaCl (32). In order to uncover the molecular mechanisms of saline resistance, we first constructed a cDNA yeast library, screened this library on potato dextrose agar supplemented with various concentrations of NaCl, and isolated a series of genes with strong saline resistance. In the present study, we focused on an aquaglyceroporin candidate, *AgGlpF*, confirming its water/glycerol transport activity, and analyzing its biological functions in different systems: *S. cerevisiae,* the model filamentous fungus *Neurospora crassa*, and the model plant *Arabidopsis thaliana*. This is the first report describing the *in planta* heterologous expression of a fungal aquaglyceroporin channel. The results of this study provide a candidate gene for genetic engineering of enhanced stress tolerance in crops and further the understanding of the regulation of salt tolerance in the halophilic fungus *A. glaucus.*

Applied and Environmental Microbiology

MATERIALS AND METHODS

Strains and culture conditions. Spores of *A. glaucus* were cultured (10^6–10^{10} spores/mL) in potato dextrose medium containing 10% NaCl at 30°C for approximately 6 days. The *E. coli* strains employed in this study were DH5α. Standard procedures were used for manipulating bacterial cells and recombinant DNA (33,34). The *S. cerevisiae* strains used in the present study were INV*Sc*1 (His-, Leu-, Trp-, and Ura-). Yeast cells were grown in yeast potato dextrose (YPD; 2% peptone, 1% yeast extract, and 2% glucose). *Neurospora crassa* were cultured in Vogel's Medium (35,36) at 30°C.

Plant materials and culture conditions. *Arabidopsis* (Columbia ecotype) seeds were surface-sterilized with 75% (v/v) ethanol for 1 min and 6% NaClO (v/v) for 5 min, and then washed with sterile water five times. The sterilized seeds were germinated in sterile water and grown in Murashige and Skoog (MS) solid medium with a 16 h light/8 h dark cycle at 25°C and a relative humidity of 70–80% for 2 weeks. These seedlings were transferred to a soil mixture of vermiculite:peat moss:perlite (1:1:1) in a greenhouse and irrigated with Hoagland's nutrient solution and allowed to grow for another 2 weeks.

Cloning of the *AgGlpF* gene from *A. glaucus* and protein sequence analysis.To select genes related to salt tolerance, a primary cDNA library from *A. glaucus* treated with NaCl was constructed in *E. coli*. Then whole cDNA library plasmids were transformed into *S. cerevisiae*. Yeast transformants were functionally screened by gradually increasing the concentration of NaCl, and transformants were obtained with a tolerance of 20% NaCl (37). The full-length cDNA sequence of the *AgGlpF* gene was

directly cloned from salt-tolerant transformants using primers (T7: 5'-TAATACGAC TCACTATAGGGA-3' and attB2: 5'-CTTTGTACAAGAAAGCTGGGT -3').

The molecular weight and isoelectronic point predictions for the deduced AgGlpF protein were performed using the computational isoelectronic point/molecular weight tool (http://www.expasy.org/tools/protparam.html). Multiple alignments of AQPs sequences (Table S1) were performed using CLUSTALW as implemented in MEGA 5.05. The phylogenetic tree was constructed using the neighbor-joining method and the stability of branch nodes was measured by performing 1,000 bootstraps.

The spatial structure prediction. The spatial structure of *AgGlpF* was predicted with the SWISS-MODEL server (http://swissmodel.expasy.org/). Figures were generated with Swiss-PdbViewer 4.1.0.

Determination of water or glycerol transport activity of the *AgGlpF* gene. The *AgGlpF* open reading frame was inserted in the *EcoRI-XhoI* site of the reconstructed pXbG-ev1 RNA expression vector. The resulting plasmid was linearized, and then mixed with caped transcription reagents (mMESSAGE mMACHINE T7 Kit, Ambion) to *in vitro* synthesize the capped cRNAs. Osmotic water or glycerol permeability assays were carried out according to Uzcategui *et al*. (38). Briefly, The tage V of *Xenopus* oocytes were stored in ND96 buffer (96 mM NaCl, 2 mM KCl, 1.8 mM CaCl2, 1 mM MgCl2, 5 mM HEPES, pH 7.4) for next use. The defolliculated oocytes were injected with 50 ng of cRNA in 50 nl RNase free water. Control oocytes were injected with the same volume of RNase free water. Then injected oocytes were incubated in ND96 buffer at 18 °C for 3 d.

To measure osmotic water permeability (*Pf-water*), the injected oocytes were transferred into 1:3 diluted ND96 buffer. To measure glycerol permeability (*Pf-glycerol*), the oocytes were transferred into iso-osmotic ND96 buffer in which 65 mM NaCl was replaced by 130 mM glycerol. Oocyte swelling were detected with video-microscopy and calculation of oocyte permeabilities for water and glycerol using the formula: $Pf = V0 \times d(V/V0)/dt[S \times Vw \times (OM_{in} - OM_{out})]$. Osmotic water permeability (*Pf*, μm/s) was calculated from the oocyte surface area (S = 0.045 cm^2), the initial slope of the relative volume increase ($d(V/V0)/dt$ in s^{-1}), the molecular water volume (Vw = 18 cm^3/mol), and the osmotic gradient (OM_{in}-OM_{out}) by the following equation:. The initial swelling rates ($d(V/V0)/dt$ in s^{-1}) were used to compare solute permeabilities.

***AgGlpF* stress tolerance assays.** The *AgGlpF* open reading frame was amplified from the *A. glaucus* cDNA library using PCR with the primer pair TScGlpF-F/TScGlpF-R (TScGlpF-F: 5'-CGGGAATTCATGCTCCATAACTTTGTTG-3', *Eco*RI site underlined; TScGlpF-R: 5'-CCGCTCGAGCATCTACTGGCTCAATCC-3', *Xho*I site underlined). The PCR-amplified product was *Eco*RI–*Xho*I digested and directionally cloned into the yeast expression vector pYES2, which contains a URA3 selection marker driven by the GAL1 promoter. The resulting plasmid was designated pYES2-*AgGlpF*. The construct was then used to transform the *S. cerevisiae* strain INV*Sc*1 (His-, Leu-, Trp-, and Ura-). Sequence analysis confirmed that the *AgGlpF* gene was inserted into the pYES2 plasmid. The INV*Sc*1 yeast strain was inoculated from colonies on YPD plates and grown for 3 days at 30°C.

Plasmid transformation with both empty pYES2 and pYES2-*AgGlpF* was performed using the lithium acetate method according to the pYES2 vector kit instructions (Invitrogen, Carlsbad, CA, USA). Yeast cells harboring pYES2-*AgGlpF* and the empty pYES2 vector (control) were incubated in SC-Ura liquid medium containing 2% glucose at 30°C overnight. The cultures were adjusted to an optical density $(OD)_{600}$ of 0.4 in 5 mL of induction medium (SC-Ura medium supplemented with 2% (w/v) galactose) and incubated at 30°C for 24 h to promote expression of the *AgGlpF* gene.

For the stress experiments, densities of yeast cells were measured (OD_{600}) after incubation, and the culture samples (cells transformed with pYES2-*AgGlpF* and the pYES2 vector control) were adjusted to an equal number of cells (OD_{600} = 1.0 in 1 mL of medium). The cells were cultured in 5 mL of medium containing 0.2%, 0.4%, 0.6%, 0.8%, and 1% $CuSO_4$ at 30°C for 24 h with shaking. For salt and drought stress, the yeast cells were cultured in 1 M, 2 M, or 3 M NaCl and 0.4 M, 0.8 M, 1.2 M, 1.6 M, or 2 M sorbitol at 30°C for 24 h with shaking. Cell densities were measured (OD_{600}) after each treatment.

Analysis of salt tolerance of *AgGlpF* in *N. crassa*. *Neurospora crassa* as a filamentous fungus is often used as an experimental model, and the method for its genetic transformation has been well refined. The homologous gene *NcAQP* (XP_965183) from *N. crassa* was obtained using BlastP comparative analysis. Using the mutant strain Δ*aqp*, complementary expression vectors (pSur-*AgGlpF* and pSur-*NcAQP*) were constructed and further transformed into the mutant strain Δ*aqp* to verify its tolerance to salt and to explore the mechanisms regulating the expression of the *AgGlpF* gene.

The expression vector introduced into *N. crassa* was constructed for expression of the *AgGlpF* gene by cloning it with the primer pair TNcGlpF-F/TNcGlpF-R. After digestion with *Xba*I and *Eco*RI, the amplified *AgGlpF* fragment was inserted into plasmid pSur, yielding plasmid pSur-*AgGlpF*. *NcAQP* was also subcloned into plasmid pSur using the same procedure with the primer pair TNcAQP-F/TNcAQP-R.

Asparagine-proline-alanine sequences (NPA motifs) play a key function in transporting water and solute. Thus, NPA-deleted *AgGlpF* complementary vectors were constructed, and NPA-deletion products were amplified with fusion PCR using six primers P1–P6. A schematic diagram for the construction of NPA-deleted *AgGlpF* products is shown in Fig. S1 and the primers used in constructing complementary vectors of transformed *N. crassa* are listed in Table S2.

The construct was transformed into *N. crassa* via electroporation methods using spores. Then transformants were screened in medium supplemented with 100 mg/mL hygromycin and verified by PCR using gene specific primers (Hyg-F/Hyg-R) with genomic DNA as a template. The wild-type (WT) strain, mutant strain Δ*aqp*, *AgGlpF* complementary strain, *NcAQP* complementary strain, *NPA1*-deletion complementary strain, *NPA2*-deletion complementary strain, and *NPA1,2*-deletion complementary strain were inoculated on Vogel's solid medium containing 10% NaCl.

Measurement of intracellular glycerol content in *N. crassa*. Mycelium blocks 5 mm in diameter from WT *N. crassa*, mutant strain *Δaqp*, and *AgGlpF* or *NcAQP* complementary strains were obtained using a round punch, inoculated in Vogel's liquid

medium, and cultured for 2 days under normal conditions. The four different mycelia were collected using three layers of gauze each and transferred into 10% or 15% NaCl in Vogel's liquid medium for 0.5h, 1 h, 2 h, 4 h, 8 h or 12 h. Untreated strains served as controls. The intracellular glycerol concentration in *N. crassa* was measured using a previously published method (39).

Expression patterns of glycerol metabolism-related genes in *N. crassa* and *A. glaucus*. In response to a salt stressor, the expression profiles of glycerol metabolism-related genes were analyzed using real-time PCR. Glycerol metabolism-related genes and primer sequences employed in this analysis are provided in Table S3.

Total RNA from each sample was extracted using TRIzol reagent (Life Technologies Corporation, Carlsbad, California, USA) in accordance with the manufacturer's instructions. Approximately 0.5 g of total RNA from each pool was reverse transcribed to cDNA in the presence of oligo-deoxythymidine in a volume of 10 μL following the protocol provided in the PrimeScript RT Reagent Kit (TaKaRa Corp, Dalian, China). The synthesized cDNA was then diluted to 100 μL with sterile water and used as the template for real-time PCR.

Real-time reverse transcriptase (RT)-PCR was conducted using a 7500 Real-Time PCR system (Applied Biosystems). To normalize the amount of total RNA present in each reaction, β-actin (XM_956040) genes were used as internal controls. PCR was performed in a total volume of 20 μL containing 10 μL of SYBR Green Real-time PCR Master Mix (Toyobo), 0.5 μM of each forward and reverse primer, and 2 μL of cDNA

template (equivalent to 100 ng total RNA). The amplification was performed using the following cycle parameters: 94°C for 30 s, followed by 45 cycles of 94°C for 12 s, 60°C for 30 s, 72°C for 40 s, and 78.5°C for 1 s for plate reading. Three independent biological repeats were performed for each treatment. Gene expression levels were calculated from the threshold cycle according to the $2^{-\Delta\Delta Ct}$ method.

Plant transformation and subcellular location analysis of *AgGlpF*. The sequencing-confirmed coding region of *AgGlpF* cDNA was cloned into the pGFPGUS*Plus* vector (40) at the *Xba*I site using the primer pair TPGlpF-F/TPGlpF-R (TPGlpF-F: 5'-GCTCTAGAATGCTCCATAACTTTGTTG-3'; TPGlpF-R: 5'-GCTCTAGATCAATCCAGTCGGAGAGC-3'), thus allowing the gene to be driven by the CaMV 35S promoter. The construct was introduced into competent cells of the *Agrobacterium tumefaciens* strain EH105 using the freeze-thaw method. The *Arabidopsis thaliana* ecotype Columbia plants were grown under 16 h light/8 h dark conditions at 22°C for transformation. The prepared plasmid construct was transformed into *Arabidopsis* plants *via* the *Agrobacterium*-mediated vacuum infiltration method previously described (41). Seeds were collected and screened in MS medium supplemented with 20 mg/mL hygromycin. Homozygous (T3 generation) transgenic *AgGlpF* plants were crossed to obtain transgenic plants. Integration and expression of these transgenes in the transgenic plants were assessed by PCR using gene specific primers (TPGlpF-F/TPGlpF-R) with genomic DNA as a template and by quantitative RT-PCR (RT-qPCR) using the total RNA isolated from leaf samples. Three independent

transgenic homozygous T3 line (TG) seedlings and the WT were used for subsequent experiments, with the *β*-tubulin gene (Forward primer: 5'-ATGTTCAGGCGCAAGGCTT-3'; Reverse primer: 5'-TCTGCAACCGGGTCATTC AT -3') used as an internal control.

To investigate the cellular localization of AgGlpF, the AgGlpF-GFP fusion protein was expressed in onion (*Allium cepa* L.) epidermal cells using the *Agrobacterium*-mediated transformation method (42). The GFP vector was used as a control. The transformed cells were cultured for 24 h at room temperature in the dark on MS medium to promote expression of the fusion protein prior to observation, and then analyzed using a confocal laser scanning microscope (model LSM410; Zeiss, Jena, Germany) with the following settings: 488 nm for excitation of GFP and 507 nm long pass for emission. Fluorescent microscopic images were collected using a fluorescence microscope.

Polyclonal antibody preparation and western blot analysis. The ORF of *AgGlpF* was amplified with the primer pair TScGlpF-F/TScGlpF-R. The PCR-amplified product was *Eco*RI–*Xho*I digested and inserted to vector pET32a (Novagen, Billerica, MA, USA) to generate a fusion protein with a hexahistidine tag. The fusion proteins were expressed in *E. coli* BL21 transformants following standard procedures. Cells were harvested by centrifugation, and disrupted by physical fragmentation. The total proteins were purified by affinity chromatography using a nickel column (Ni-NTA agarose, Roche). The purified

Applied and Environmental Microbiology

286 protein was injected into rabbits to produce primary polyclonal antibodies as previously
287 described (37).

288 The total proteins extracted from each of corresponding samples were denatured in
289 the SDS-PAGE loading buffer at 95°C for 10 min. Western blot analysis was performed
290 using the antiserum against AgGlpF and visualized with an enhanced horseradish
291 peroxidase-diaminobenzidine (HRP-DAB) substrate kit (Tiangen, Beijing China). The
292 conserved protein β-tubulin was used as an internal control. Polyclonal antibody against
293 β-tubulin was purchased from Qiangyao Peptide Company (Shanghai, China).

294 **Germination and seedling growth assays.** For germination assays, seeds were
295 sterilized for 1 min with 70% (v/v) ethanol and 5 min with 6% NaClO (v/v), followed by
296 several rinses with sterile distilled water, and then maintained at 4°C in the dark for 2
297 days. Fifty seeds of each transgenic line and the WT were placed on the MS agar medium
298 (0.6%) supplemented with 150 mM NaCl or 350 mM mannitol, and then transferred to a
299 controlled environment (16 h of light at 22°C and 8 h of dark at 18°C). The germination
300 rate was calculated after the seeds were in the controlled environment for 7 days.

301 For early growth assessments, 5-day-old WT plants and three transgenic line
302 seedlings were placed on MS agar medium containing various concentrations of NaCl
303 and mannitol (0 mM, 100 mM, or 200 mM). *Arabidopsis* plants were grown vertically
304 under normal conditions. The root lengths were measured after 1 week.

305 **Salt and drought treatments of transgenic *Arabidopsis* plants.** Three 5-week-old
306 transgenic *Arabidopsis* lines (TL1, TL2, and TL45) and WT plants were subjected to

various abiotic stress treatments. Thirty plants of each line were used for drought stress and 30 plants of each line were used for salt stress treatments. For salt stress, plants were irrigated with Hoagland's nutrient solution containing 350 mM NaCl for 3 weeks, and then returned to the original growth conditions for 2 weeks. The survival rate was calculated. For drought stress, water was withheld from the plants for 3 weeks before water was once again introduced. Two weeks later, the survival rate was calculated.

RESULTS

Isolation and characterization of *AgGlpF*. We selected genes conferring salt resistance by screening the *A. glaucus* cDNA library in *S. cerevisiae* on YPD solid medium supplemented with 10%, 15%, or 20% NaCl, on which WT yeast strains cannot survive. The cDNA fragments inserted from the salt-tolerant transformants were identified by PCR amplification and then sequenced (accession number: AHZ59733). The full-length cDNA for *AgGlpF* was isolated from *A. glaucus* and determined to be 1,218 base pairs (bp) in length. The 5'- and 3'-untranslated regions (UTR) were 249 and 108 bp in length, respectively. The open reading frame was 861 bp and encoded a 287 amino acid protein with a calculated molecular weight of 31.1 kDa. Conserved protein domains were analyzed using Basic Local Alignment Search Tool (BLAST; National Center for Biotechnology Information) alignment. The results showed that *AgGlpF* contained six transmembrane domains at amino acid positions 20–39, 48–65, 96–118, 158–177, 190–212, and 239-261, and two conserved NPA signature motifs of the AQP family at amino acid positions 72–74 and 212–214 (Fig. S1). The spatial structure of the

AgGlpF protein was predicted using the SWISS-MODEL server with the *E. coli* GlpF channel (PDB ID: 1fx8) serving as a template (Fig. S2). Although the sequence identity was 40.53%, the monomeric and tetrameric structures of AgGlpF and *E. coli* GlpF were especially similar (Fig. S2), indicating a resemblance to the glycerol transporter.

The evolutionary relationships among the various species of AQPs were examined to provide insight into their functional evolution. Thirty-seven AQPs in different fungi species were used for alignment analysis with the AgGlpF protein (Fig. 1). The result indicated that the AgGlpF protein shared an amino acid identity up to 94% with the GlpF protein in *Aspergillus ruber*, and with other *Aspergillus* strains, the identity was greater than 76%, suggesting that AgGlpF is a member of the third aquaglyceroporins subgroup.

Both Water and glycerol transport activities of AgGlpF in *Xenopus laevis* Oocytes. The major function of GlpFs is water transport channel, which has been widely detected in most organisms (1,2). The water transport activity test for AgGlpF was performed in the membrane transport experimental system *Xenopus laevis* oocytes. As a result, the AgGlpF injection in *Xenopus* oocytes led to a 7-fold increase of the osmotic water permeability coefficient in comparison with water injection (Fig. 2A). As mentioned in the introduction, GlpFs may transport glycerol or other small uncharged solutes. Therefore, the glycerol permeability coefficient value of AgGlpF-expressing oocytes (Pf-glycerol) was measured. As expected, oocytes expressing AgGlpF showed a 6-fold higher Pf-glycerol value than the water-injected oocytes (Fig. 2B), confirming that AgGlpF functions as a aquaglyceroporin with both water and glycerol transport activities.

***AgGlpF* improves osmotic tolerance in yeast.** To validate the stress tolerance of AgGlpF, two types of transformed yeast were generated. One was transformed with the plasmid of pYES2-AgGlpF, and the other was transformed with an empty pYES2 as a control. AgGlpF proteins expressed in yeast transformants were determined using western blot analysis (Fig. 3A). The two types of yeast cells were treated with different osmotic stresses to determine whether expression of AgGlpF confers osmotic stress tolerance to transgenic yeast. The result demonstrated that there was no difference in growth between these two kinds of yeast under normal culture conditions (Fig. 3B). By contrast, yeast cells harboring pYES2-*AgGlpF* exhibited increased survival rates relative to the control under NaCl (Fig. 3C), sorbitol (Fig. 3D), and $CuSO_4$ (Fig. 3E), confirming *AgGlpF* is associated with high osmosis tolerance under selected stressors.

***AgGlpF* with two NPA motifs is important for high salt tolerance in *N. crassa*.** *Neurospora crassa* as a model fungus is convenient for genetic manipulation. In order to analyze the salt tolerant ability of *AgGlpF*, several complementary transformants containing expression vectors (pSur-AgGlpF, pSur-NcAQP, and three *NPA*-deleted *AgGlpFs*) were created based on the *NcAQP* disruption mutant (*Δaqp*) of *N. crassa*. The results indicated that the Δ*aqp* strain was barely alive on Vogel's solid medium supplemented with 10% NaCl, but the *NcAQP* complementary strain, like the wild type, was still alive (Fig. 4A). Interestingly, the *AgGlpF* complementary strain grew faster than the wild type or the *NcAQP* complementary strain (Fig. 4A), clearly demonstrating that

AgGlpF is more resistant to salt stress than *NcAQP* is. The AgGlpF proteins expressed in the selected transformants of *N. crassa* were analyzed using western blot (Fig 4B).

Asparagine-proline-alanine sequences (NPA motifs) play a key role in transporting water, glycerol or other solutes. Three individual NPA-deleted *AgGlpF* fragments were amplified with fusion PCR using six primers (P1–P6) and inserted into their respective complementary vectors (Fig. S1). Each *NPA*-deleted *AgGlpF* was transferred into the deletion strain Δ*aqp*. Salt resistance was analyzed on the same medium containing 10% NaCl. The results demonstrated that each of the *NPA*-deletion complementary strains grew on the salt medium, but tolerance in each of these strains was weaker than that in the Δ*aqp/AgGlpF*, Δ*aqp/NcAQP*, or wild type (Fig. 4A), suggesting that the individual *NPA* sites are important for salt resistance. Here, it's worth mentioning that in Fig. 4B, three protein bands similar to AgGlpF in molecular weight were detected in lanes of *Δnpa1*, *Δnpa1*, and *Δnpa1*,2. The weaker signals could be due to lower level of expression of proteins with deletions; alternatively, NPA deletions affected the binding of the antibodies.

AgGlpF promotes intracellular glycerol accumulation in *N. crassa*. Intracellular glycerol is a compatible solute for maintaining intracellular osmolality. We investigated whether the accumulation of intracellular glycerol is associated with AgGlpF expression. The results showed that under salt stress, the intracellular glycerol concentration of the *AgGlpF* complementary strain (Δ*aqp*/AgGlpF) was significantly higher than that of the WT, mutant strain (Δ*aqp*), and *NcAQP* complementary strain (Δ*aqp*/NcAQP) (Fig. 5A).

Moreover, with the increase of salt concentration, the intracellular glycerol accumulation also increased (Fig. 5B).

AgGlpF localized on the cell membrane enhances osmotic tolerance in plants. GlpFs are cell membrane channel proteins. According to the deduced amino acid sequence, *AgGlpF* contains six transmembrane domains. To investigate its subcellular localization in a plant, a transient expression onion system was applied. The *AgGlpF*-GFP fusion protein (Fig. 6A) and the GFP protein were respectively introduced into onion epidermal cells. Following 24–48 h of transformation, confocal laser scanning microscopy was used to examine the cells. As a result, the *AgGlpF*-GFP fusion protein was expressed and localized on the cell membrane of onion epidermal cells (Fig. 6B), indicating that *AgGlpF* functions in plant.

Therefore, the role of *AgGlpF* in drought stress tolerance was further investigated by generating transgenic *Arabidopsis* plants overexpressing *AgGlpF* under the control of the CaMV 35S promoter (Fig. 6A). A total of 48 transgenic lines (T1) were screened by their resistance to hygromycin and confirmed with PCR using primers specific to AgGlpF and GFP (data not shown). Among the T1 lines, three transgenic lines (TL1, TL2 and TL45) segregated with a ratio of 3:1 for hygromycin resistance. In addition, all the three independent transgenic T2 line seedlings survived on MS medium containing 20 mg/L of hygromycin. Transgenic T3 line seedlings were confirmed using RT-qPCR and western blot (Fig. 7A). In this experiment, WT or transgenic plants harboring vacant vector lines served as a negative control and were subjected to the same analysis. *Arabidopsis* seed

411 germination was examined after the seeds were sown on MS medium supplemented with
412 various concentrations of mannitol or NaCl. Germination rates of control and TG seeds
413 showed no significant difference on normal MS medium (data not shown). However, as
414 shown in Fig. 7B, when seeds were germinated on 150 mM NaCl for 7 days, only 24.33%
415 germination was seen in the WT line, whereas the three TG lines, TL1, TL2 and TL45,
416 showed 85%, 80%, and 80.3% germination, respectively. Under mannitol stress, the
417 percentage germination over 7 days for the WT was much lower than that of the TG lines.
418 When the seeds of WT and TG lines were germinated in the presence of 350 mM
419 mannitol, the germination rates of the TG lines (TL1, 81.33%; TL2, 72.67; TL45, 81.67%)
420 were higher than those of the WT plants (20.33%) (Fig. 7C).

421 *Arabidopsis* seedlings are sensitive to certain concentrations of NaCl or mannitol.
422 As the concentration of NaCl or mannitol increased, the root lengths of the control lines
423 were significantly arrested. 5-day-old WT plants and three transgenic line seedlings were
424 placed on MS agar medium containing various concentrations of NaCl and mannitol (0,
425 100, or 200 mM). As shown in Fig. 8A, the growth was significantly different between
426 the WT line and TG lines for the various treatments. Under 100 mM and 200 mM NaCl
427 treatments, the roots were approximately twofold longer for transgenic lines than for WT
428 plants (Fig. 8B). However, the roots were approximately fourfold longer for AgGlpF
429 transgenic lines than for WT plants grown in media containing 100 mM and 200 mM
430 mannitol, respectively (Fig. 8C). Thus, overexpression of AgGlpF in *Arabidopsis*
431 increased tolerance to NaCl and mannitol stressors during seed germination and root

growth. Above all, in comparison to the resistance to salt, *AgGlpF* appeared to be more resistant to drought stress (Fig. 8C).

Plants that grow with higher survival rates, normal size or/and fewer yellow leaves are considered more tolerant to stressors. To mimic the performance of AgGlpF transgenic lines under drought and salt stress in natural field, the three TG lines and the controls, were planted in soil. Compared with the WT plants under normal conditions, TG *Arabidopsis* plants showed no apparent phenotypic difference before treatment; however, under stress conditions, the TG plants did show differences. After 2 weeks of exposure to 350 mM NaCl, most of the leaves in the TG lines remained green, whereas leaves of the WT plants turned yellow, and most of the WT plants withered and died (Fig. 9A). After 3 weeks of drought, the WT plants were undersized and more withered than TG plants. By contrast, TG plants began bolting during the same time (Fig. 9C). The TG lines exhibited higher survival rates than WT lines under both drought and salt stressors (Fig. 9B and 9D). The results further verified that overexpression of *AgGlpF* can enhance salt and drought tolerance, implying a great application potential in osmotic resistant genetic engineering.

DISCUSSION

GlpFs belong to a superfamily of major intrinsic proteins that are membrane water/glycerol channels involved in many physiological processes. Filamentous fungal aquaglyceroporins are still poorly characterized at both the molecular and the cellular levels. The halophilic fungus *A. glaucus*, which was isolated from air-dried wild

453 vegetation at the surface periphery of a solar salt field, shows extreme salt tolerance, with
454 a salinity range for growth up to 32% NaCl (32). Therefore, GlpF of *A. glaucus* is a good
455 candidate for use in achieving a deeper understanding of the physiological roles of
456 aquaglyceroporins in fungi. In this study, the *AgGlpF* gene was isolated by screening a
457 cDNA library of *A. glaucus* in yeast cells. Yeast cells overexpressing *AgGlpF* displayed
458 markedly enhanced tolerance to salt, drought, and heavy metal stressors, indicating that
459 *AgGlpF* is involved in tolerance to osmotic or other abiotic stress.

460 The sequence identity of aquaporins share limited similarity and differ in size, but
461 the reported X-ray structures of aquaporins, such as bovine AQP0, human AQP1, *E. coli*
462 AqpZ and GlpF, spinach SoPIP2;1, and *Plasmodium falciparum* PfAQP, show that these
463 proteins share a conserved overall typical hourglass model (43-45). AQPs are assembled
464 as homotetramers consisting of four independent monomers embedded in the lipid bilayer
465 (46). Each monomer comprises six membrane-spanning α-helices (H1–6) connected by
466 five loops (A–E), with both amino and carboxyl termini located in the cytoplasm (47).
467 The NPA signature motifs are located at the ends of the two short α-helices (loops B and
468 E), and are thought to be critical to water and substrate permeation (44). The two highly
469 conserved NPA signature motifs are also contained in the AgGlpF protein (Fig. S1); and
470 the spatial structure prediction of the AgGlpF protein clearly shows the typical aquaporin
471 structure (Fig. S2). Given the water/glycerol transport activities in *Xenopus* oocytes (Fig.
472 2) and the high levels of glycerol accumulated in cells of Δ*aqp/AgGlpF* (Fig. 4), AgGlpF
473 is no doubt one of the glycerol transporters. In fact, the attribute of the AgGlpF can also

be interpreted from the analysis of osmotic stress tolerance among the series of *N. crassa* strains: the Δ*aqp* strain lost growth ability under salt stress (10% NaCl); and the *NPA*-deletion complementary strain exhibited weaker salt tolerance than the complementary strains of the full-length *AgGlpF* (Fig. 4).

The osmoregulatory mechanism has been extensively studied in the yeast *S. cerevisiae*. Upon hyperosmotic shock, the high osmolarity glycerol (HOG) signaling pathway, one of the best understood MAPK cascades, is activated to control glycerol accumulation (19). Hog1 kinase stimulates transcription of genes encoding the enzymes required for glycerol biosynthesis, glycerol-3-phosphate dehydrogenase (Gpd1) and glycerol 3-phosphatase (Gpp2) (48,49) as well as glycerol import (via the glycerol/H^+ symporter Stl1) (50). Hog1 kinase also activates a regulatory enzyme in glycolysis (Pfk26/27). In the mean time, the Fps1 glycerol channel rapidly closes to prevent glycerol outflow (15,18). Both the extremely halotolerant yeast *Hortaea werneckii* and the halophilic fungus *Wallemia ichthyophaga* accumulate glycerol to adapt to hyperosmotic conditions. The levels of glycerol are increased with increasing salinity and decreased after hypoosmotic shock (51,52). Several genes known to be involved in glycerol production were found in the genomes of *H. werneckii* and *W. ichthyophaga* (53). Among these genes, there are three aquaglyceroporins homologue to *AgGlpF*. Considering the hyperosmotic resistant ability of these fungi, and that the *AgGlpF* complementary strain of *N. crassa* was more resistant to salt and had significantly higher intracellular glycerol content than the WT, Δ*aqp,* and *NcAQP* complementary strains (Fig. 5), thus, we

hypothesized that the enhanced resistance to salt stress may be due to the accumulation of intracellular glycerol.

Intracellular glycerol accumulation is dependent on glycerol synthesis, transport, and retention, as well as on tightly regulated events. Thus, we analyzed the expression of glycerol metabolism-related genes in *N. crassa* and *A. glaucus* using RT-qPCR. The mitogen-activated protein kinase gene (*MAPK*) and *AgGlpF* were rapidly induced and reached a maximum 2 h after treatment with NaCl in *A. glaucus* (Fig. S3A). However, in *N. crassa*, the induced *NcMPK* and NcAQP peaked at 4 h after treatment with NaCl, though the expression patterns of both genes were so similar (Fig. S3B). Upon hyperosmotic shock, *GPD1* and *GUP1* were also induced by NaCl in both fungi; however, the expression level of *NcGPD1* was lower and the response to hyperosmotic shock was slower than those for MAPK and *AgGlpF* or *NcAQP*. At this point, it appeared to be that MAPK and *AgGlpF* are mainly responsible for this accumulation of glycerol.

This report describes the overexpression of the aquaglyceroporin gene *AgGlpF* from the halophilic fungus *A. glaucus* in *Arabidopsis* plants as well as in fungal species. It also demonstrated the subsequent phenotypic characterization of this transgenic plant during salt and drought stress. While transgenic methods to explore the role of plant AQPs have been reported previously (54-56), this is the first report describing the in planta heterologous expression of an aquaglyceroporin derived from a filamentous fungus. Recently, a viral aquaglyceroporin of *Chlorovirus* (*aqpv1*) has been expressed in tobacco (57). In the report, the transgenic tobacco plant performed better under drought conditions

and showed faster recovery following re-watering than control plants, indicating a role for a heterologous aquaglyceroporin in mitigating drought stress (57). In the present study, overexpressing *AgGlpF* markedly enhanced tolerance to high salt and drought in transgenic *Arabidopsis* plants. Thus, our results provide an even better candidate gene for genetic engineering of enhanced stress tolerance in crops.

The halophilic fungus of *A. glaucus* may be a rich genetic pool for cloning osmotic resistance genes, because in our previous research, we screened and discovered so many resistant genes, such as *AgRPL44* (37) and *AgRPS3aE* (58) in the halophilic fungus *A. glaucus*. In conclusion, our findings advance the understanding of the molecular mechanisms of salt tolerance in filamentous fungal cells and offer important insights in the breeding of new stress-resistant crops.

ACKNOWLEDGMENTS

We thank Dr. Hon-Ming Lam at The Chinese University of HongKong for discussions and technical advice. The project was supported by the National Natural Science Foundation of China (31171794), Ministry of Agriculture of China (2011ZX08009-001).

REFERENCES

1. **Madeira A, Moura TF, Soveral G**. 2015. Aquaglyceroporins: implications in adipose biology and obesity. Cell Mol Life Sci. **72:** 759 -771.

2. **Engel A, Stahlberg H**. 2002. Aquaglyceroporins: channel proteins with a conserved core, multiple functions, and variable surfaces. Int Rev Cytol. **215**:75–104.

536 3. **Heller KB, Lin EC, Wilson TH**. 1980. Substrate specificity and transport properties
537 of the glycerol facilitator of *Escherichia coli*. J Bact. **144**: 274–278.
538 4. **Maurel C, Reizer J, Schroeder JI, Chrispeels MJ, Saier MHJr**. 1994. Functional
539 characterization of the *Escherichia coli* glycerol facilitator, GlpF, in *Xenopus* oocytes. J
540 Biol Chem. **269**: 11869–11872.
541 5. **Agre P, Bonhivers M, Borgnia MJ**. 1998. The aquaporins, blueprints for cellular
542 plumbing systems. J Biol Chem. **273**: 14659–14662.
543 6. **Borgnia M, Nielsen S, Engel A, Agre P**. 1999. Cellular and molecular biology of the
544 aquaporin water channels. Annu Rev Biochem. 68: 425–458.
545 7. **Heymann JB, Engel A**. 1999. Aquaporins: phylogeny, structure, and physiology of
546 water channels. Physiology. **14**: 187–193.
547 8. **Agre P, King LS, Yasui M, Guggino WB, Ottersen OP, Fujiyoshi Y, Engel A,**
548 **Nielsen S**. 2004. Aquaporin water channels from atomic structure to clinical medicine.
549 J Physiol. **542**: 3–16.
550 9. **Lee JK, Khademi S, Harries W, Savage D, Miercke L, Stroud RM**. 2004. Water and
551 glycerol permeation through the glycerol channel GlpF and the aquaporin family. J
552 Synchrotron Radiat. **11**: 86–88.
553 10. **Carbrey JM, Agre P**. 2009. Discovery of the Aquaporins and Development of the
554 Field Aquaporins.Beitz, E., editor. Springer; Berlin Heidelberg: pp. 3–28.

555 11. **Fu D, Libson A, Miercke LJ, Weitzman C, Nollert P, Krucinski J, Stroud RM**.
556 2000. Structure of a glycerol-conducting channel and the basis for its selectivity.
557 Science. **290**: 481–486.
558 12. **Pettersson N, Filipsson C, Becit E, Brive L, Hohmann S**. 2005. Aquaporins in
559 yeasts and filamentous fungi. Biol Cell. **97**: 487–500.
560 13. **Xu H, Cooke JEK, Zwiazek JJ**. 2013. Phylogenetic analysis of fungal aquaporins
561 provide insight into their possible role in water transport of mycorrhizal associations.
562 Botany-Botanique. **91:** 495–504.
563 14. **Verma RK, Prabh ND, Sankararamakrishnan R**. 2014. New subfamilies of major
564 intrinsic proteins in fungi suggest novel transport properties in fungal channels:
565 implications for the host-fungal interactions. BMC Evol Biol. **14**:173.
566 15. **Tamás MJ, Luyten FC, Sutherland A, Hernandez J, Albertyn J, Valadi H, Li H,**
567 **Prior BA, Kilian SG, Ramos J, Gustafsson L, Thevelein JM, Hohmann S**. 1999.
568 Fps1p controls the accumulation and release of the compatible solute glycerol in yeast
569 osmoregulation. Mol Microbiol. **31**: 1087–1104.
570 16. **Oliveira R, Lages F, Silva-Graça M, Lucas C**. 2003. Fps1p channel is the mediator
571 of the major part of glycerol passive diffusion in *Saccharomyces cerevisiae*: artefacts
572 and re-definitions. Biochim Biophys Acta. **1613**: 57–71.
573 17. **Hohmann I, Bill RM, Kayingo I, Prior BA**. 2000. Microbial MIP channels. Trends
574 Microbiol. **8**: 33–38.

18. **Luyten K, Albertyn J, Skibbe WF, Prior BA, Ramos J, Thevelein JM, Hohmann S**. 1995. Fps1, a yeast member of the MIP family of channel proteins, is a facilitator for glycerol uptake and efflux and is inactive under osmotic stress. EMBO J. **14**: 1360–1371.

19. **Hohmann S, Krantz M, Nordlander B**. 2007. Yeast osmoregulation. Methods Enzymol. 428: 29–45.

20. **Ahmadpour D, Geijer C, Tamás MJ, Lindkvist-Petersson K, Hohmann S**. 2014. Yeast reveals unexpected roles and regulatory features of aquaporins and aquaglyceroporins. Biochim Biophys Acta. **1840**: 1482–1491.

21. **Li T, Hu YJ, Hao ZP, Li H, Chen BD**. 2013. Aquaporin genes *GintAQPF1* and *GintAQPF2* from *Glomus intraradices* contribute to plant drought tolerance. Plant Signal Behav. **8**: e24030. doi: 10.4161/psb.24030.

22. **Dietz S, von Bülow J, Beitz E, Nehls U**. 2011. The aquaporin gene family of the ectomycorrhizal fungus *Laccaria bicolor*: lessons for symbiotic functions. New Phytol. **190**: 927–940.

23. **Nehls U, Dietz S**. 2014. Fungal aquaporins: cellular functions and ecophysiological perspectives. Appl Microbiol Biotechnol. **98**: 8835–8851.

24. **Birch E**. 2013. Aquaporins in *Magnaporthe oryzae*. University of, Oxford.

25. **Thines E, Weber RWS, Talbot NJ**. 2000. MAP kinase and protein kinase A-dependent mobilization of triacylglycerol and glycogen during appressorium turgor generation by *Magnaporthe grisea*. Plant Cell. **12**: 1703–1718.

596 26. **Srivastava AK, Penna S, Nguyen DV, Tran LS**. 2014. Multifaceted roles of
597 aquaporins as molecular conduits in plant responses to abiotic stresses. Crit Rev
598 Biotechnol. **28**: 1–10.
599 27. **Dean RM, Rivers RL, Zeidel ML, Roberts DM**. 1999. Purification and functional
600 reconstitution of soybean nodulin 26. An aquaporin with water and glycerol
601 transport properties. Biochemistry. **38**: 347–353.
602 28. **Echevarria M, Windhager EE, Tate SS, Frindt G**. 1994. Cloning and expression of
603 AQP3, a water channel from the medullary collecting duct of rat kidney. Proc Natl
604 Acad Sci U S A. **91**: 10997–11001.
605 29. **Ma T, Frigeri A, Hasegawa H, Verkman AS**. 1994. Cloning of a water channel
606 homolog expressed in brain meningeal cells and kidney collecting duct that functions
607 as a stilbene-sensitive glycerol transporter. J Biol Chem. **269**: 21845–21849.
608 30. **Hatakeyama S, Yoshida Y, Tani T, Koyama Y, Nihei K, Ohshiro K, Kamiie**
609 **JI,Yaoita E, Suda T, Hatakeyama K, Yamamoto T**. 2001. Cloning of a new
610 aquaporin (AQP10) abundantly expressed in duodenum and jejunum. Biochem
611 Biophys Res Commun. **287**: 814–819.
612 31. **Mobasheri A, Shakibaei M, Marples D**. 2004. Immunohistochemical localization of
613 aquaporin 10 in the apical membranes of the human ileum: a potential pathway for
614 luminal water and small solute absorption. Histochem Cell Biol. **121**: 463–471.
615 32. **Liu XD, Liu JL, Wei Y, Tian YP, Fan FF, Pan HY, Zhang SH**. 2011. Isolation,
616 dentification and Biologic Characteristics of an Extreme Halotolerant *Aspergillus* sp.

617 J. Jilin Univ. **49**:548–552. (In Chinese; abstract in English.) http://www.cnki.
618 com.cn/Article/CJFDTotal-JLDX201103039.htm.
619 33. **Sambrook J, Fritsch EF, Maniatis T**. 1989. Molecular Cloning: A Laboratory
620 Manual, 2nd edn, Cold Spring Harbor Laboratory Press, Plainview, New York.
621 34. **Ausubel F, Brent R, Kingston RE, Moore DD, Seidman JG., Smith JA, Struhl K**.
622 1999. Short Protocols in Molecular Biology, 4th edn, New York.
623 35. **Vogel HJ**. 1956. A convenient growth medium for *Neurospora* (Medium N).
624 Microbial Genet Bull. **13**: 42–43.
625 36. **Vogel HJ**. 1964. Distribution of lysine pathways among fungi: Evolutionary
626 implications. Am Nat. **98**: 435–446.
627 37. **Liu XD, Xie LX, Wei Y, Zhou XY, Jia BL, Liu JL, Zhang SH**. 2014. Abiotic stress
628 resistance, a novel moonlighting function of ribosomal protein RPL44 in the
629 halophilic fungus *Aspergillus glaucus*. Appl Environ Microbiol. **80**: 4294–4300.
630 38. **Uzcategui NL, Szallies A, Pavlovic-Djuranovic S, Palmada M, Figarella K,**
631 **Boehmer C, Lang F, Beitz E, Duszenko M.** 2004. Cloning, heterologous expression,
632 and characterization of three aquaglyceroporins from *Trypanosoma brucei*. J Biol
633 Chem. **279**: 42669-42676.
634 39. **Ben-Amotz A, Avron M**. 1973. The role of glycerol in the osmotic regulation of the
635 halophilic alga *Dunaliella parva*. Plant Physiol. **41**: 875–878.

636 40. **Vickers CE, Schenk PM, Li D, Mullineaux PM, Gresshoff PM**. 2007.
637 pGFPGUS*Plus*, a new binary vector for gene expression studies and optimising
638 transformation systems in plants. Biotechnol Lett. **29**:1793–1796.
639 41. **Tague BW, Mantis J**. 2006. In planta Agrobacterium-mediated transformation by
640 vacuum infiltration. Methods Mol Biol. **323**: 215–223.
641 42. **Sun W, Cao ZY, Li Y, Zhao YX, Zhang H**. 2007. A simple and effective method
642 for protein subcellular localization using Agrobacterium-mediated transformation of
643 onion epidermal cells. Biologia. **62**: 529–532.
644 43. **Bhattacharjee H, Mukhopadhyay R, Thiyagarajan S, Rosen BP**. 2008.
645 Aquaglyceroporins: ancient channels for metalloids. J Biol. **7**: 33.
646 44. **Jung JS, Preston GM, Smith BL, Guggino WB, Agre P**. 1994. Molecular structure
647 of the water channel through aquaporin CHIP. The hourglass model. J Biol Chem.
648 **269**: 14648–14654.
649 45. **Walz T, Hirai T, Murata K, Heymann JB, Mitsuoka K, Fujiyoshi Y, Smith BL,**
650 **Agre P, Engel A**. 1997. The three-dimensional structure of aquaporin-1. Nature. **387**:
651 624–627.
652 46. **Smith BL, Agre P**. 1991. Erythrocyte Mr 28,000 transmembrane protein exists as a
653 multisubunit oligomer similar to channel proteins. J Biol Chem. **266**: 6407–6415.
654 47. **Tani K, Fujiyoshi Y**. 2014. Water channel structures analysed by electron
655 crystallography. Biochim Biophys Acta. **1840**: 1605–1613. doi:10.1016/j.bbagen.
656 2013.10.007

48. **Albertyn J, Hohmann S, Thevelein JM, Prior BA**. 1994. GPD1, which encodes glycerol 3-phosphate dehydrogenase, is essential for growth under osmotic stress in *Saccharomyces cerevisiae*, and its expression is regulated by the high osmolarity glycerol response pathway. Mol Cell Biol. **14**: 4135–4144.

49. **Pahlman AK, Granath K, Ansell R, Hohmann S, Adler L.** 2001. The yeast glycerol 3-phosphatases gpp1p and gpp2p are required for glycerol biosynthesis and differentially involved in the cellular responses to osmotic, anaerobic, and oxidative stress. J Biol Chem. **276**: 3555–3563.

50. **Ferreira C, van Voorst F, Martins A, Neves L, Oliveira R, Kielland-Brandt M C, Lucas C, Brandt A.** 2005. A member of the sugar transporter family, Stl1p is the glycerol/H^+ symporter in *Saccharomyces cerevisiae*. Mol Biol Cell. **16**: 2068–2076.

51. **Kogej T, Stein M, Volkmann M, Gorbushina AA, Galinski EA, Gunde-Cimerman N**. 2007. Osmotic adaptation of the halophilic fungus *Hortaea werneckii*: role of osmolytes and melanization. Microbiology. **153**: 4261–4273.

52. **Zajc J, Kogej T, Galinski EA, Ramos J, Gunde-Cimerman N**. 2014. Osmoadaptation strategy of the most halophilic fungus, *Wallemia ichthyophaga*, growing optimally at salinities above 15% NaCl. Appl Environ Microbiol. **80**: 247–256.

53. **Plemenitaš A, Lenassi M, Konte T, Kejžar A, Zajc J, Gostinčar C, Gunde-Cimerman N**. 2014. Adaptation to high salt concentrations in halotolerant /halophilic fungi: a molecular perspective. Front Microbiol. **5**: 199.

678 54. **Wang X, Li Y, Ji W, Bai X, Cai H, Zhu D, Sun X, Chen LJ, Zhu YM**. 2011. A
679 novel *Glycine soja* tonoplast intrinsic protein gene responds to abiotic stress and
680 depresses salt and dehydration tolerance in transgenic *Arabidopsis thaliana*. J Plant
681 Physiol. **168**:1241–1248.
682 55. **Zhou SY, Hu W, Deng XM, Ma ZB, Chen LH, Huang C, Wang C, Wang J, He**
683 **YZ, Yang GX, He GY**. 2012. Overexpression of the wheat aquaporin gene, TaAQP7,
684 enhances drought tolerance in transgenic tobacco. PLoS One. **7**: e52439. doi:
685 10.1371/journal.pone.0052439.
686 56. **Kumar K, Mosa KA, Chhikara S, Musante C, White JC, Dhankher OP**. 2014.
687 Two rice plasma membrane intrinsic proteins, OsPIP2;4 and OsPIP2;7, are involved
688 in transport and providing tolerance to boron toxicity. Planta. **239**: 187–198.
689 57. **Bihmidine S, Cao M, Kang M, Awada T, Van Etten JL, Dunigan DD, Clemente**
690 **TE.** 2014. Expression of Chlorovirus MT325 aquaglyceroporin (aqpv1) in tobacco
691 and its role in mitigating drought stress. Planta. **240**: 209–221.
692 58. **Liang X, Liu Y, Xie L, Liu X, Wei Y, Zhou X, Zhang SH.** 2015. A ribosomal protein
693 AgRPS3aE from halophilic Aspergillus glaucus confers salt tolerance in heterologous
694 organisms. Int J Mol Sci. **16**: 3058-3070.

Figure legends

FIG 1 Phylogenetic tree of aquaporins from selected fungi. The multiple alignments generated by ClustalW and the phylogenetic tree were constructed with MEGA 5.05 using a bootstrap test of phylogeny with the minimum evolution test and default parameters. The strains and GenBank accession numbers of fungal aquaporin proteins used for drawing the phylogenetic tree are shown in S1 Table.

FIG 2 Water/glycerol transport activity of AgGlpF. (A) Osmotic water permeability coefficient (*Pf-water*) of oocytes injected with cRNA of *AgGlpF* or water. (B) Glycerol permeability coefficient (*Pf-glycerol*) of oocytes injected with cRNA of *AgGlpF* or water. The Pf values were calculated from the rate of oocyte swelling. The data represent means ± SD of three experiments. Significant differences between oocyte cells containing the cRNA of *AgGlpF* and control are indicated as $*p < 0.05$ or $**p < 0.01$. Three biological experiments were performed, which produced similar results.

FIG 3 Stress tolerance analysis in AgGlpF-overexpressing yeast cells. (A) Western blot analysis of AgGlpF protein in yeast cells. Total proteins extracted from the wild-type strain pYES2 and pYES2- AgGlpF strains; AgGlpF was detected with an anti-AgGlpF antibody, and the presence of β-tubulin was detected as an internal control; The experiment was performed twice, and a representative blot is presented. (B-E) Stress tolerance analysis. Yeast cells were cultured in YPD liquid medium (B), or in YPD liquid medium supplemented with NaCl (C), sorbitol (D), and CuSO4 (E); The data represent

means ± SD of three experiments. Significant differences between yeast cells containing pYES2-*AgGlpF* and control are indicated as $*p < 0.05$ or $**p < 0.01$.

FIG 4 Salt tolerance analysis of AgGlpF in *N. crassa*. (A) Salt-tolerant phenotypes of various *N. crassa* strains grown on Vogel's medium containing 10% NaCl. (B) Western blot analysis. Equal amounts of protein were loaded in each lane on one gel. AgGlpF was detected with an anti-AgGlpF antibody, and the presence of β-tubulin was detected as an internal control; The experiment was performed twice, and a representative blot is presented. Δ*aqp* indicates *NcAQP* deletion mutant strain; Δ*aqp/AgGlpF* indicates *AgGlpF* complementary strain; Δ*aqp/NcAQP* indicates *NcAQP* complementary strain; Δnpa1, Δnpa1, and Δnpa1,2 indicate the three NPA-deleted *AgGlpFs* complementary strains.

FIG 5 Intracellular glycerol content of various *N. crassa* strains. (A) Treatment with 1.7M (10%) NaCl. (B) Treatment with 2.6M (15%) NaCl. WT indicates wild type strain; Δ*aqp* indicates mutant strain; Δ*aqp/AgGlpF* indicates *AgGlpF* complementary strain; Δ*aqp/NcAQP* indicates *NcAQP* complementary strain. Significant differences between the Δ*aqp*/AgGlpF strain and other three strains are indicated as $*p < 0.05$, $**p < 0.01$.

FIG 6 AgGlpF-GFP fusion protein was subcellularlly localized on the cell membrane. (A) Schematic diagram for the construction of the expression vector used for plant transformation. (B) Subcellular localization of *AgGlpF* in onion epidermal cells. Scale bars in all panels are 50 μm.

FIG 7 Transgenic *Arabidopsis* plants overexpressing AgGlpF and their seed germination under osmotic stress. (A) Detection of *AgGlpF* expression using RT-PCR (the up panel) and Western blot (the low panel) with β -tubulin as an internal control. (B,C) Germination rates of *Arabidopsis* plants overexpressing the *AgGlpF* gene in the presence of stressors.

FIG 8 Salt and drought tolerance in transgenic *Arabidopsis* seedlings. (A) Salt and drought tolerance phenotype of *Arabidopsis* overexpressing *AgGlpF*. (B,C) Root lengths of *Arabidopsis* plants overexpressing the *AgGlpF* gene in the presence of stressors. Data represent means ± SD of three experiments. Significant differences between the TG lines and control (WT) are indicated as $*p < 0.05$, $**p < 0.01$.

FIG 9 The enhanced salt and drought tolerance in transgenic *Arabidopsis* planting in soil . (A) Phenotypes of WT and TG lines after 2 weeks of NaCl treatment. (B) Survival rates after NaCl treatment. (C) Phenotypes in WT and TG lines after 3 weeks of drought. (D) Survival rates after the drought treatment. Data represent means ± SD of three experiments. Significant differences between the TG lines and control (WT) are indicated as $**p<0.01$.

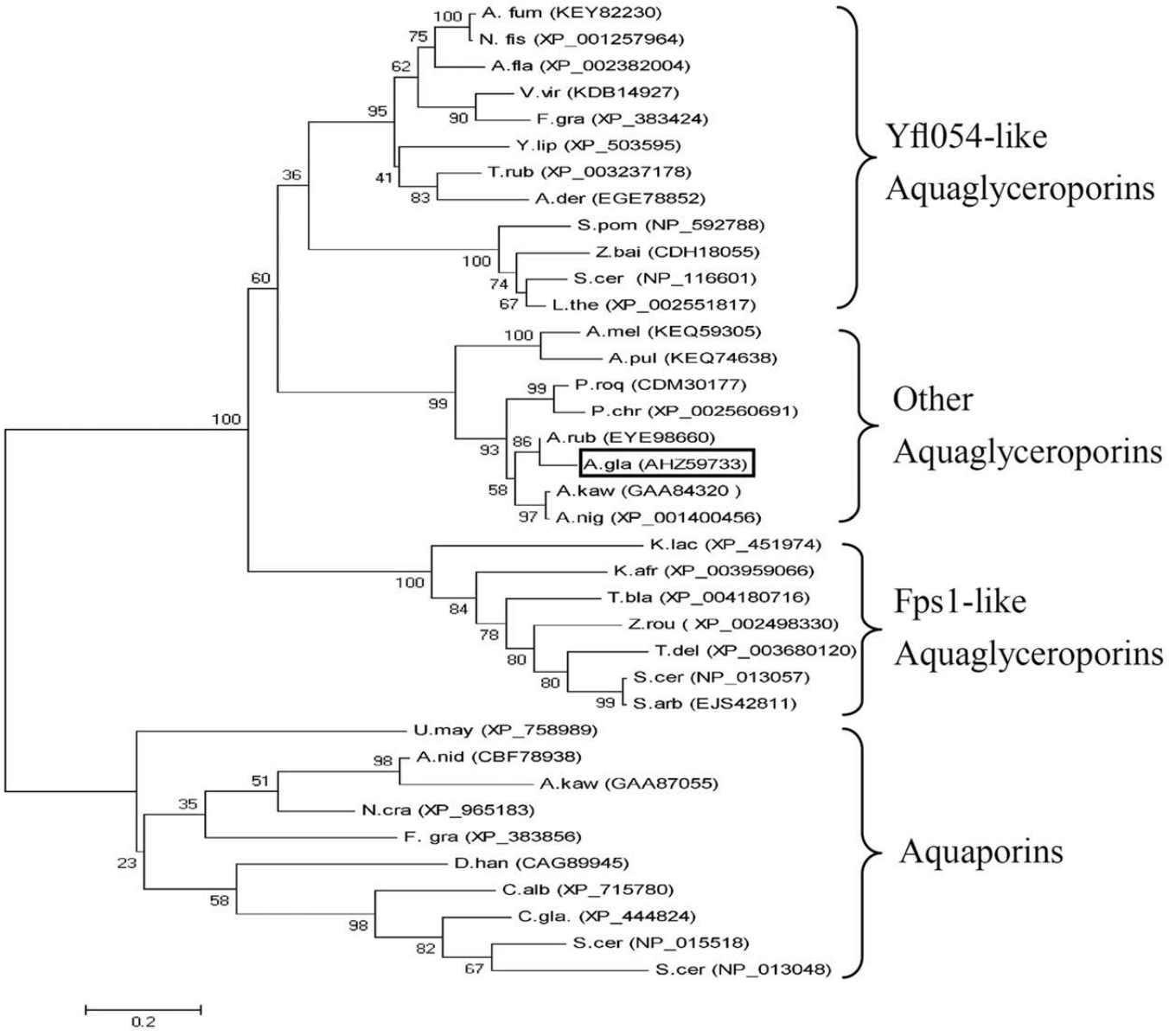

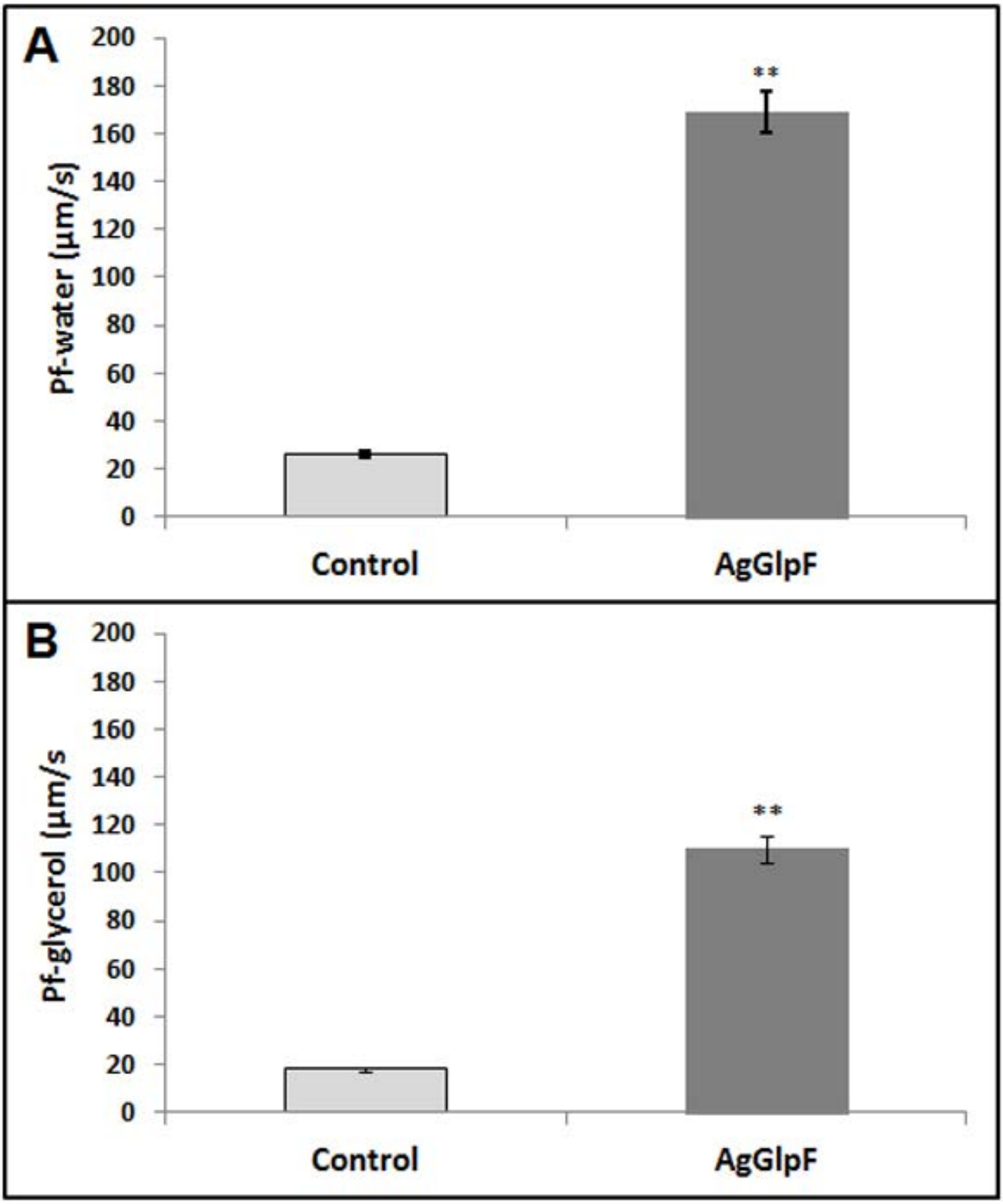

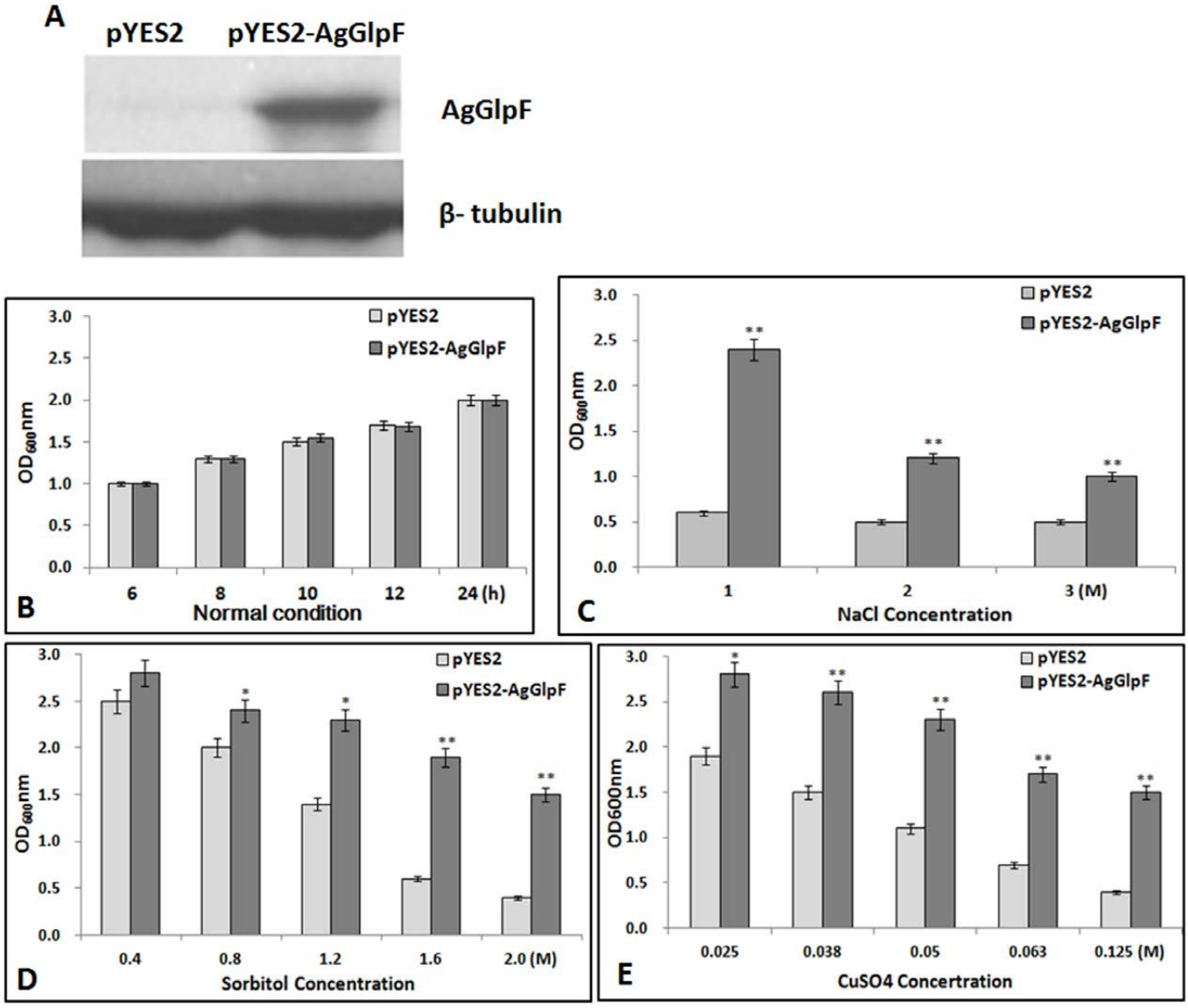

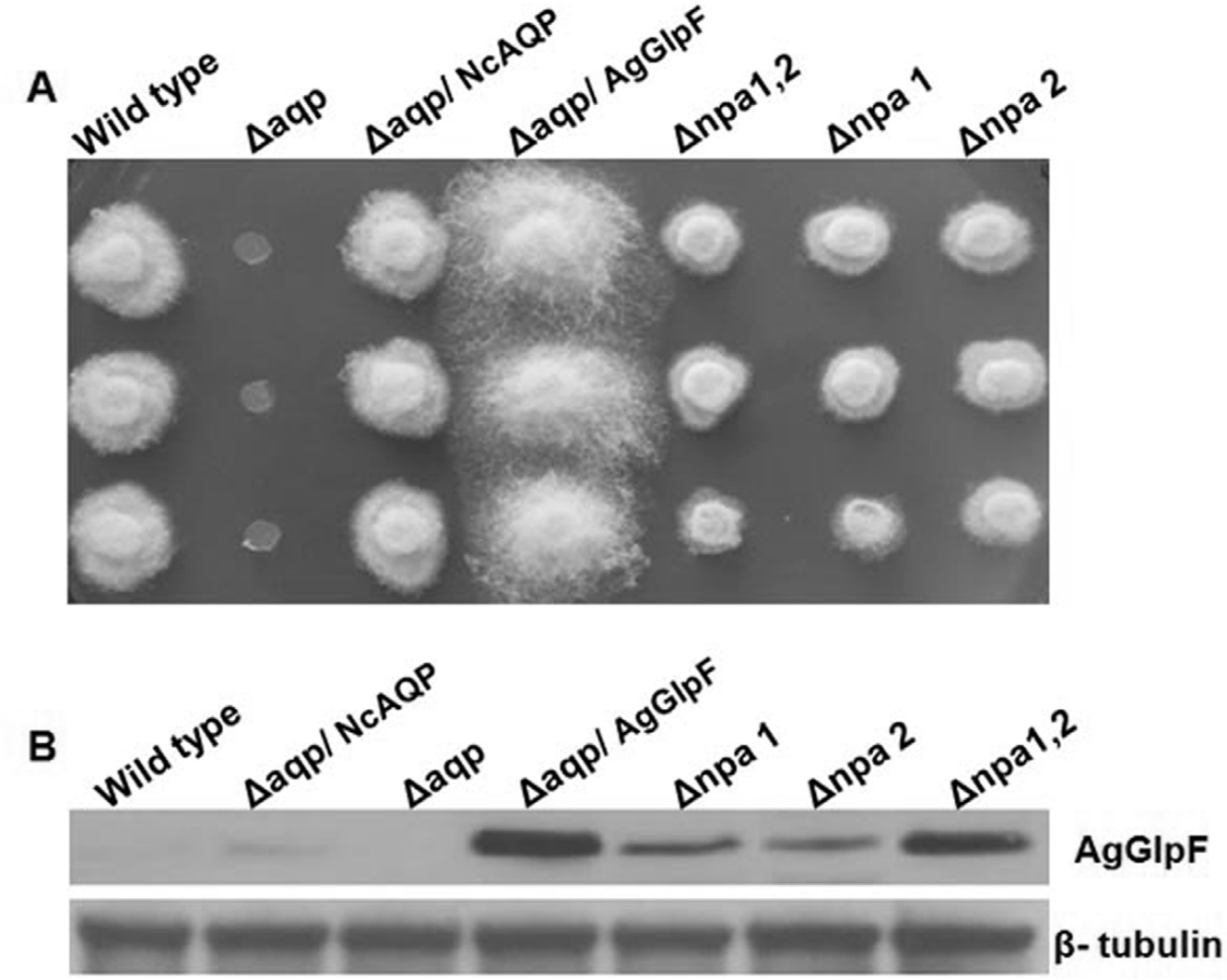

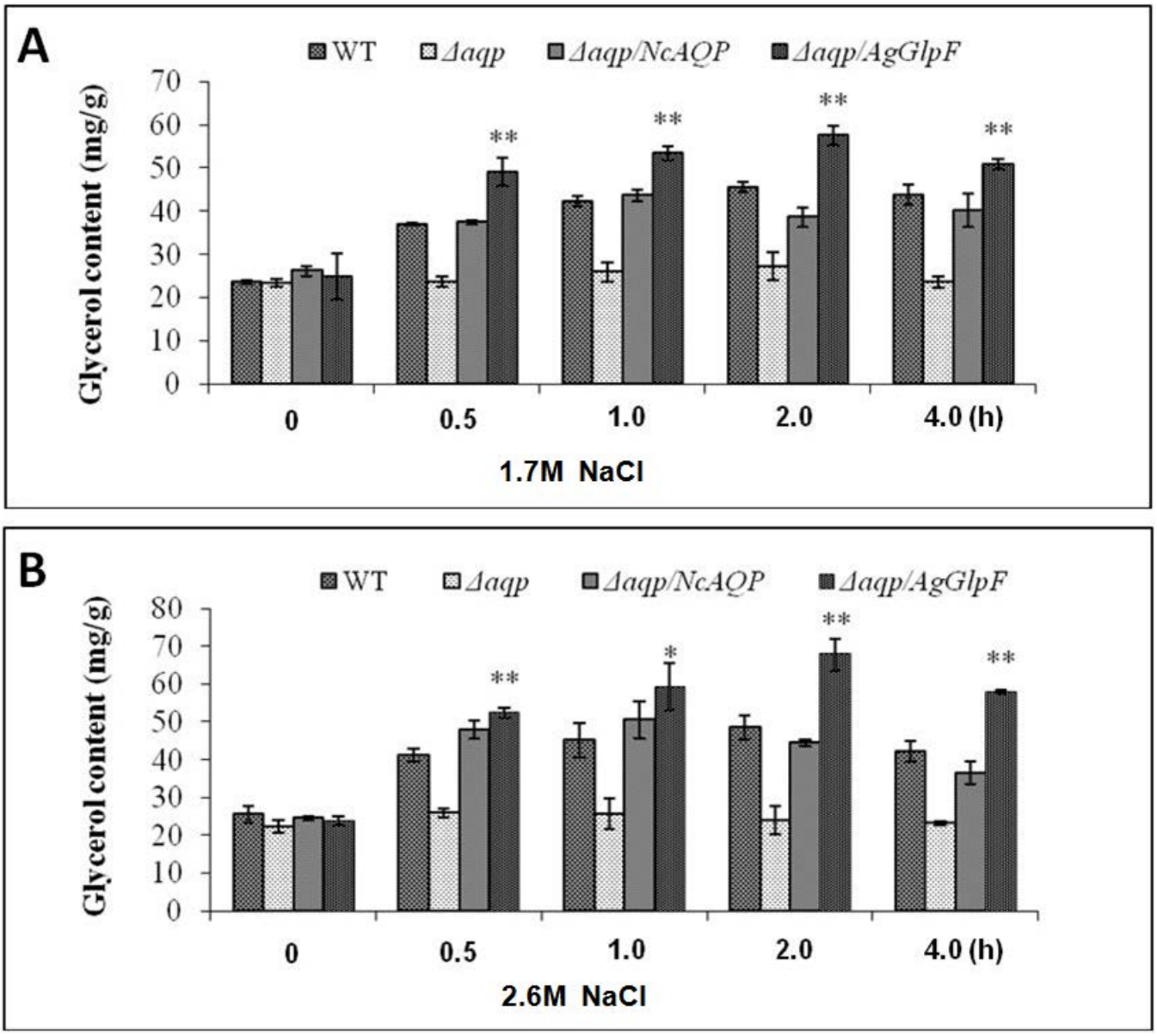

Applied and Environmental Microbiology